

Information Measures for Long-Range Correlated Sequences: the Case of the 24 Human Chromosome Sequences

A. Carbone^{1,2,3,*}

¹*Politecnico di Torino, Italy*

²*ISC-CNR, Unità Università di Roma 'La Sapienza', Italy*

³*ETH Zurich, Switzerland*

Abstract

The Shannon (block) entropy of the clusters generated by intersecting a long-range correlated sequence with its moving average is studied. The entropy is given by two terms, respectively increasing *logarithmically* and *linearly* (besides a constant term), corresponding to clusters with power-law or exponentially distributed lengths. Then, the entropy measure is implemented on the 24 human chromosome sequences. Interestingly, it is found that, for the power-law correlated clusters, the nucleotide composition is, on the average, equal to the nucleotide composition of the whole sequence, while, for the exponentially correlated clusters, it fluctuates around the average value. Even more interestingly, it is found that the variance of the fluctuations is a characteristic property of each chromosome. How these fluctuations correlate to biological properties such as segmental duplications, gene density of each chromosome is finally discussed.

PACS numbers:

*Electronic address: anna.carbone@polito.it

I. INTRODUCTION

Complex systems are probed by observing a relevant quantity over a certain temporal or spatial range, yielding long-range correlated sequences or arrays, with the remarkable feature of displaying ‘ordered’ patterns, which emerge from the seemingly random structure. The degree of ‘order’ is intrinsically linked to the information embedded in the patterns, whose extraction and quantification might add clues to many complex phenomena [1–7].

In this work, we put forward an information measure for long-range correlated sequences, worked out from a partition of the sequence into words or blocks (here called *clusters*) according to [6]. The clusters are characterized by their length ℓ , duration τ and area \mathcal{A} , obeying power-law probability distributions, with a cross-over to an exponential decay at large size. Further information measures based on this partition approach and extension to higher dimensions might be envisaged for future development [7, 8].

The probability distribution function of the lengths is considered to estimate the Shannon (block) entropy of the clusters. It is shown that the entropy can be written as the sum of three terms: a constant, a logarithmic and a linear function of the cluster length. The clusters with dominant logarithmic term of the entropy are power-law correlated and correspond to ‘ordered’ structures, while those with dominant linear term are exponentially distributed and correspond to ‘disordered’ structures.

The information measure is illustrated by analyzing the 24 nucleotide sequences of the human chromosomes [9]. Each sequence is first mapped to a fractional Brownian walk (the so-called DNA walk). Then, the probability distribution function $P(\ell)$ and the entropy $S(\ell)$ of the DNA clusters are estimated by adopting the aforeproposed approach. It is shown that the power-law correlated clusters are characterized by a nucleotide content (in terms of purine-pyrimidine pairs (G+C)% and (A+T)%) on the average equal to the value of the whole chromosome sequence. Conversely, the exponentially correlated clusters are characterized by a percentage of purine-pyrimidine pairs exhibiting fluctuations around the value of the whole chromosome sequence. Interestingly, it is shown that the variance σ_C of the cluster composition fluctuations for each of the 24 chromosomes is correlated to biologically relevant properties, such as duplication frequency and gene density. It should be pointed out that the entropy of a sequence, coded in blocks or words, has been extensively studied since its introduction by Shannon (see [2–4] and Refs. therein). The novelty of the

present approach resides in the method used for partitioning the sequence in words, which provides the set of inherently correlated ones in a straightforward manner.

II. METHOD

A random sequence $y(x)$ can be partitioned in elementary clusters by considering the intersection with the moving average $\tilde{y}_n(x)$ where n is the size of the moving window. The clusters correspond to the regions bounded by $y(x)$ and $\tilde{y}_n(x)$ between two subsequent crossings points $x_c(i)$ and $x_c(i+1)$ [6]. The intersection between $y(x)$ and $\tilde{y}_n(x)$ produces a *generating* partition, yielding different sequences of clusters for different values of n .

The probability distribution function $P(\ell, n)$ of the lengths ℓ for each n can be obtained by counting the clusters $\mathcal{N}(\ell_1, n), \mathcal{N}(\ell_2, n), \dots, \mathcal{N}(\ell_i, n)$ respectively with length $\ell_1, \ell_2, \dots, \ell_i$. By doing so, one obtains:

$$P(\ell, n) \sim \ell^{-D} \mathcal{F}(\ell, n) \sim \mu(\ell, n)^{-1} , \quad (1)$$

where $D = 2 - H$ is the fractal dimension of the sequence and the function $\mathcal{F}(\ell, n)$ can be taken of the form:

$$\mathcal{F}(\ell, n) \equiv \exp(-\ell/n) . \quad (2)$$

$\mathcal{F}(\ell, n)$ accounts for the drop-off of $P(\ell, n)$ due to finiteness of n when $\ell \gg n$. The quantity $\mu(\ell, n) = \ell^D \exp(\ell/n)$ corresponds to the size of the cluster lengths spanned by the random walkers. $\mu(\ell, n)$ ranges from a line proportional to ℓ for $H = 1$ to a square proportional to ℓ^2 for $H = 0$ respectively. The probability distribution function $P(\ell, n)$ is shown in Fig. 1 for a wide range of n values, estimated for a long range correlated series with Hurst exponent $H \approx 0.6$. For $n \rightarrow 1$, the lengths ℓ of the elementary clusters are centered around a single value. When n increases, a broader range of lengths is obtained and, consequently, $P(\ell, n)$ spreads over all values.

The Shannon (block) entropy is defined as [2–4]:

$$S(\ell, n) \equiv - \sum_{\mu(\ell, n)} P(\ell, n) \log P(\ell, n) , \quad (3)$$

where the sum is performed over all the elementary clusters. By using Eq. (1) and Eq. (3), the cluster entropy writes:

$$S(\ell, n) = S_0 + \log \ell^D - \log \mathcal{F}(\ell, n), \quad (4)$$

which, after taking into account Eq. (2), becomes:

$$S(\ell, n) = S_0 + \log \ell^D + \frac{\ell}{n} , \quad (5)$$

where S_0 accounts for the constant terms, $\log \ell^D$ is related to the term ℓ^{-D} and ℓ/n is related to the term $\mathcal{F}(\ell, n)$.

To clarify the meaning of the terms appearing in Eq. (5), it is worthy of remarking that for isolated systems, the entropy increase is related to the irreversible processes spontaneously occurring within the system. It tends to a constant value as a stationary state is asymptotically reached ($dS \geq 0$). For open systems interacting with their environment, the entropy increase is given by a term $dS_i \geq 0$, due to the irreversible processes spontaneously occurring within the system, and a term dS_e due to the irreversible processes arising through external interactions. The term $\log \ell^D$ in Eq. (5) should be interpreted as an intrinsic entropy S_i . It is independent of the method of partitioning the sequence (which plays the role of the external interaction) and in particular of n . The logarithmic term is of the form of the Boltzmann entropy $S = \log \Omega$, where Ω is the maximum volume occupied by the isolated system. The quantity ℓ^D corresponds to the volume occupied by the random walker. Whenever ℓ could reach the maximum size L of the sequence, the second term on the right side writes $\log L^D$. The term ℓ/n represents the excess entropy S_e introduced by the partition process. It comes into play when the long-range correlated sequence is partitioned in clusters and depends on n .

Fig. 2 shows the entropy $S(\ell, n)$ evaluated by using the probability distribution $P(\ell, n)$ plotted in Fig. 1. One can note that $S(\ell, n)$ increases logarithmically at small ℓ , while it increases as a linear function at larger ℓ , as expected according to Eq. (5). In particular, $S(\ell, n)$ behaves as $\log \ell^D$ and is n -invariant for small values of ℓ . Clusters with lengths ℓ greater than n are not power-law correlated, due to the finite-size effects introduced by the window n . They are characterized by a value of the entropy exceeding the values lying on the curve $\log \ell^D$. Clusters with a given length ℓ can be generated by different values of the window n . For example, clusters with $\ell = 2500$ have entropies corresponding to the point A (for $n = 1000$) or A'' (for $n = 3000$ and $n = 10000$) as shown in Fig. 2. One can observe that A'' corresponds to power-law correlated (i.e. ordered) clusters, since A'' lies on the curve $\log \ell^D$. Conversely, the point A does not correspond to power-law correlated clusters, since A lies on the curve ℓ/n which originates from the term $\mathcal{F}(\ell, n)$. In other words, clusters with

lengths shorter than n are ordered (long-range correlated), whereas clusters with lengths larger than n are disordered (exponentially correlated).

To gain further insight in the meaning of the terms appearing in Eq. (5), the *source entropy rate* s , is calculated for the entropy $S(\ell, n)$. The *source entropy rate* is a measure of the excess randomness of the coding algorithm. Noisy coding processes are characterized by large values of s [2]. By using the definition and Eq. (5), the *source entropy rate* writes:

$$s \equiv \lim_{\ell \rightarrow \infty} \frac{S(\ell, n)}{\ell} = \frac{1}{n} . \quad (6)$$

The excess randomness of the clusters is inversely proportional to n and, thus, becomes negligible in the limit of $n \rightarrow \infty$. This can be clearly observed in the curves of Fig. 2, where one can note that higher entropy rates correspond to steeper slopes of the linear term ℓ/n .

A. Application: the 24 Human Chromosome Sequences.

The publication of several completely sequenced genomes from many species provides a unique opportunity to develop suitable statistical methods and yield benchmarks for the identification of biological features [9–29].

The two strands of DNA are held together by hydrogen bonds between complementary bases: two bonds for the AT pair and three bonds for the GC pair, which is therefore stronger. The existence of GC-rich and GC-poor segments may have different biological role in biological processes as duplication, segmentation, unzipping. For example, the distributions of genes and repetitive elements were found to be associated with particular GC contents. Small and medium sized genes were found to be more abundant in GC-rich regions of human genome, whereas long genes (typically genes with long introns) were found to be scarce in GC rich regions.

Nonuniformity of nucleotides composition within genomes was revealed several decades ago by thermal melting and gradient centrifugation. On the basis of findings concerning buoyant densities of melted DNA fragments, a theory for the structure of genomes of warm-blooded vertebrates known as the *isochores theory* was put forward. Isochores were defined as long genomic segments that are fairly homogeneous in their guanine and cytosine (GC) composition. Though it is widely accepted that the human genome contains large regions of distinctive GC content, the availability of fully sequenced DNA or RNA molecule allows

one to accurately calculate the local properties by statistical methods. The development of efficient algorithms achieving deep and accurate description of genomes.

In this section, the information metrics described above are implemented on genomic sequences. The main computational steps are described here following.

The sequence of the nucleotide bases ATGC (FASTA file) are mapped according to the following rule: if the base is a purine (A,G), the base is mapped to +1, otherwise if the base is a pyrimidine (C,T), the base is mapped to -1 (Fig. 3). The sequence of +1 and -1 is summed and a random walk $y(x)$ (*DNA walk*) is obtained (Fig. 3).

The function $\tilde{y}_n(x)$ is calculated for the *DNA walk* with different values of the window n . The intersection between $y(x)$ and $\tilde{y}_n(x)$ yields a set of clusters. Each cluster corresponds to a segment between two adjacent intersections at $x_c(i)$ and $x_c(i+1)$ of $y(x)$ and $\tilde{y}_n(x)$. Since each cluster of the *DNA walk* corresponds to a cluster of nucleotides, the number of nucleotides ATGC is counted in each cluster. The ATGC count is plotted as a function of the cluster length ℓ . In Figs. 4-6 the nucleotide composition of the clusters is shown for the 24 human chromosomes. The nucleotide composition is plotted as a function of the cluster length ℓ for three values of n : namely $n = 2$, $n = 4$ and $n = 10$. However, the range of n values used in this work varied from 2 to 10,000. One can observe that the nucleotides count is roughly constant for clusters having length comparable or shorter than n . This means that ‘ordered’ DNA clusters, i.e. with constant nucleotide composition, are found, when the entropy varies as a logarithm of ℓ . For cluster length ℓ comparable or larger than n , the power-law correlation breakdown with the onset of exponentially correlated clusters (‘disordered’ clusters). An even more interesting results of our computation is that the amplitude of the fluctuations is not constant but they assume a characteristic value for each chromosome. For example, one can note in Figs. 4-6 the fluctuations of the cluster composition is very small for Chromosomes 8, 9, 17, Y. Conversely, they are quite large for Chromosomes 14, 15, X. The next step is addressed to understanding whether the nucleotide fluctuations, characterizing each chromosome, are linked to biological features. To this purpose, the variance σ_C of the fluctuations has been calculated for the nucleotide composition ATGC of the clusters (values are in Table II). The variances σ_C have then be correlated to other characteristic features of each chromosome: length, gene density, inter-chromosomal duplications, intra-chromosomal duplications, local ATGC composition. The correlation coefficients ρ_C are shown in Table III. Negative correlations between σ_C

and intra-and inter-chromosomal duplications are found. Strong positive correlations are observed between σ_C and AT-rich regions. These results might point to the important result that the cluster fluctuations are a fingerprint of recent segmental duplications. Dup

Conclusions

We have further developed an information measure based on the approach put forward in Refs [6, 7] and the concept of Shannon (block) entropy. The proposed approach is particularly appealing thanks to the novelty and effectiveness of the *partitioning method* for generating the blocks. The entropy writes as the sum of two contributions: one increasing *logarithmically* and the other *linearly* with the lengths of the blocks or words.

Furthermore, it has been shown that the variance of the clusters with fluctuating composition is related to relevant biological quantities like segmental duplications and AT-rich regions. The algorithm performs the following tasks: (i) separation of blocks according to their length and correlation degree; (ii) separation of DNA segments according to the nucleotide composition. Compared to already existing techniques to identify segments with certain nucleotide contents, the present method is able to give the requested output even with extremely short sequences (as shown in the plots of Figures 4 -7). Last but not least, the proposed procedure is able to identify DNA segments correlated to important biological processes-such as intra- and inter-chromosomal segmental duplications.

References

-
- [1] M. Scheffer *et al.*, Nature **461**, 7260 53 (2009); S.R. Carpenter and W.A. Brock, Ecology Letters **9** 311 (2006).
 - [2] J.P. Crutchfield, Nature Phys. **8**, 17 (2012); J.P. Crutchfield and D.P. Feldman, Chaos, **13**, 25 (2003).
 - [3] C. Wang, & B.A. Hubermann, Sci. Rep. **2**, 633 (2012).
 - [4] P. Grassberger and I. Procaccia, Phys. Rev. Lett. **50**, 346 (1983).
 - [5] C.R. Shalizi, K.L. Shalizi, R. Haslinger, Phys. Rev. Lett. **93**, 118701 (2004).

- [6] A. Carbone, G. Castelli and H. E. Stanley, Phys. Rev. E **69**, 026105 (2004); A. Carbone and H.E. Stanley, Physica A **384**, 21 (2007).
- [7] S. Arianos and A. Carbone, J. Stat. Mech: Theory and Experiment **P03037** (2009); A. Carbone, Phys. Rev. E **76**, 056703 (2007); C. Türk, A. Carbone, B.M. Chiaia Phys. Rev. E **81**, 026706 (2010).
- [8] Shao, Y., *et al.*, Sci. Rep. **2**, 835 (2012).
- [9] E.C. Lander *et al.*, Nature **409**, 860 (2001).
- [10] J.A. Bailey *et al.*, Science **297**, 1003 (2002).
- [11] P. Deloukas *et al.*, Science **282**, 744 (1998).
- [12] W. Lee, *et al.*, Nature Genetics **39**, 1235 (2007).
- [13] Y.O. Popov and A.V. Tkachenko, Phys. Rev. E **76**, 021901 (2007).
- [14] G. Bernardi, Proc. Natl. Acad. Sci. U.S.A. **104**, 8385 (2007); G. Bernardi, Gene **276**, 3 (2001).
- [15] M. Costantini, O. Clay, F. Auletta, G. Bernardi, Genome Research **16**, 536 (2006).
- [16] O. Clay, Gene **276**, 33 (2001).
- [17] N. Cohen, T. Dagan, L. Stone and D. Graur, Mol. Biol. Evol. **22**, 1260 (2005).
- [18] R. Versteeg, *et al.*, Genome Res. **13**, 1998 (2003).
- [19] M. Emanuel, *et al.*, Phys. Biol. **6**, 025008 (2009).
- [20] K.R. Bradnam, C. Seoighe, P.M. Sharp, K.H. Wolfe, Mol. Biology and Evolution **16**, 666 (1999).
- [21] R. Kapri and S.M. Bhattacharjee, Phys. Rev. Lett. **98**, 098101 (2007); J. Phys.: Cond. Matt. **18**, S215 (2006).
- [22] C. Vaillant, B. Audit, A. Arneodo, Phys. Rev. Lett. **99**, 218103 (2007).
- [23] R.K. Azad, P. Bernaola-Galvan, R. Ramaswamy, J.S. Rao, Phys. Rev. E **65**, 051909 (2002).
- [24] W. Li Phys. Rev. Lett. **86**, 5815 (2001); W. Li, Gene **276**, 57 (2001); Li W. Physica D **75** 392 (1994).
- [25] W. Salerno, P. Havlak, and J. Miller, Proc. Natl. Acad. Sci. U.S.A. **103**, 13121 (2006).
- [26] C. K. Peng *et al.*, Nature **356**, 6365, (1992), C.K. Peng *et al.*, Phys. Rev. E **49**, 1685 (1994); S.V. Buldyrev, *et al.*, Phys. Rev. Lett. **71**, 1776 (1993).
- [27] R. Roman-Roldan, P. Bernaola-Galvan, J.L. Oliver, Phys. Rev. Lett. **80**, 1344 (1998).
- [28] Z. Ouyang, J.-K. Liu, and Z.-S. She, Phys. Rev. E **72**, 041915 (2005).
- [29] S. Akhter, *et al.*, Sci. Rep. **3**, 1033 (2013).

TABLE I: Length L (2^{nd} column), Hurst exponent H (3^{rd} column), base composition (% of ATCG, 4^{th} - 7^{th} columns) of the 24 chromosomes sequences. Base composition (% of the ATCG, 8^{th} - 11^{th} columns) of the first 10MBases of the 24 chromosome sequences.

CHR	L	H	A [%]	C[%]	G[%]	T[%]	A[%]	C[%]	G[%]	T[%]
1	226217758	0.64	29.09	20.87	20.87	29.14	26.52	25.79	25.58	25.15
2	237900011	0.66	29.84	20.11	20.13	29.90	28.50	24.51	22.34	29.81
3	195304882	0.66	30.14	19.84	19.84	30.16	28.46	21.77	21.50	28.65
4	187941502	0.66	30.87	19.11	19.12	30.88	34.47	19.80	22.86	30.28
5	177847050	0.66	30.20	19.74	19.77	30.27	29.97	24.86	19.70	36.43
6	169100547	0.65	30.18	19.80	19.81	30.19	29.97	21.23	21.73	28.27
7	155403473	0.66	29.60	20.38	20.36	29.63	28.85	21.79	27.09	22.93
8	143332430	0.65	29.90	20.06	20.06	29.86	29.51	20.61	20.85	29.03
9	120994158	0.67	29.35	20.65	20.64	29.33	27.91	21.83	21.38	28.76
10	131739836	0.65	29.19	20.79	20.78	29.22	31.15	19.94	19.47	29.44
11	131247160	0.68	29.20	20.77	20.79	29.21	28.97	22.23	25.08	26.85
12	130304143	0.67	29.59	20.40	20.39	29.60	30.66	22.85	24.19	29.62
13	95747346	0.66	30.69	19.26	19.26	30.77	33.94	20.95	21.82	33.88
14	88290585	0.67	29.44	20.41	20.46	29.67	33.94	20.95	21.82	33.88
15	81927784	0.66	28.89	21.13	21.10	28.86	32.64	21.69	20.74	33.00
16	78990748	0.67	27.53	22.35	22.44	27.66	29.17	24.30	22.89	31.49
17	79620483	0.65	27.17	22.81	22.76	27.22	25.36	24.80	24.73	24.87
18	74660927	0.67	30.09	19.87	19.90	30.12	25.36	24.80	24.73	24.87
19	56038018	0.66	25.79	24.14	24.20	25.86	32.65	21.61	23.15	30.64
20	59505758	0.66	27.76	22.02	22.09	28.10	29.01	24.09	19.02	36.45
21	35452914	0.65	29.68	20.39	20.44	29.46	32.27	19.25	21.18	27.29
22	35059666	0.65	26.08	23.98	23.95	25.96	28.30	22.93	24.63	24.92
X	152580014	0.65	30.20	19.73	19.76	30.26	32.88	20.86	25.39	28.01
Y	25654723	0.72	29.88	19.87	20.08	30.14	27.45	22.05	24.21	26.49

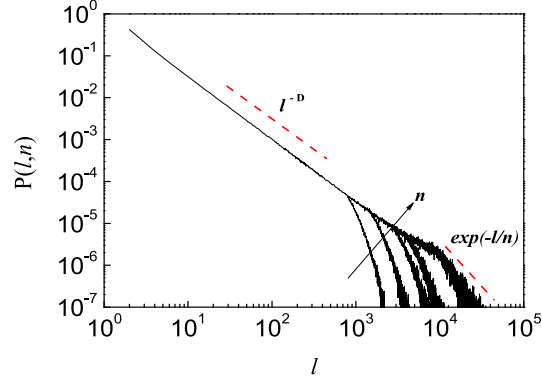


FIG. 1: Probability distribution function $P(\ell, n)$ of cluster lengths for a sequence with $H \approx 0.6$ and $L = 2^{20}$. The moving average windows are $n = 500$, $n = 1000$, $n = 2000$, $n = 3000$ and $n = 10000$ (from left to right). As n increases, $P(\ell, n)$ becomes broader. The slope of the distribution becomes steeper for $\ell > n$, corresponding to the onset of finite-size effects and exponentially decaying correlation.

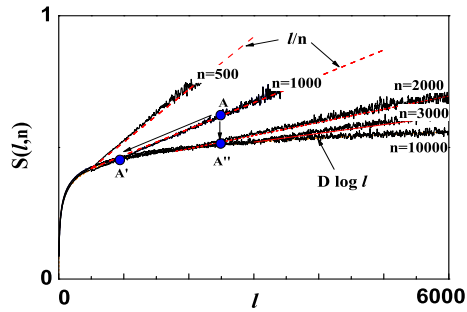


FIG. 2: Entropy $S(\ell, n)$ of the clusters according to the PDFs $P(\ell, n)$ plotted in Fig. 1.

TABLE II: Variance σ_C of the cluster composition fluctuations plotted in Figures 4,5,6,7 (% of the ATCG nucleotides) for the 24 chromosome sequences.

CHR	σ_C [A]	σ_C [C]	σ_C [G]	σ_C [T]
1	11.01	10.81	10.06	9.68
2	14.19	12.90	12.43	14.30
3	10.05	9.43	8.29	8.52
4	16.56	12.91	13.87	17.79
5	19.75	14.32	12.76	16.69
6	9.07	6.33	7.42	8.71
7	8.58	8.32	11.14	10.21
8	4.89	3.88	4.33	4.91
9	6.49	4.97	4.36	5.23
10	10.84	9.04	7.52	9.38
11	9.12	8.83	11.69	10.87
12	17.09	14.86	14.13	15.63
13	17.12	12.01	13.78	18.11
14	19.53	13.06	13.43	19.26
15	16.55	14.08	12.54	16.61
16	16.31	15.60	15.77	15.69
17	5.06	5.17	4.95	5.67
18	20.02	13.98	14.10	18.47
19	17.90	14.88	13.99	17.10
20	17.31	13.86	14.33	18.70
21	10.84	7.69	8.50	10.81
22	8.40	5.81	5.53	8.48
X	18.06	14.09	14.87	19.06
Y	6.19	6.66	7.08	7.47

TABLE III: Correlation ρ_C of the cluster variances σ_C for the first 10Mbases (M_1), the second 10Mbases (M_2) and the third 10Mbases (M_3) of the Human 24 chromosomes. The cluster variance σ_C is anticorrelated with length, gene density, inter-chromosomal and intra-chromosomal segmental duplications. The cluster variance σ_C exhibits a positive correlation with AT-rich regions. Very little correlation is found with GC-rich region and global AT composition.

	$\rho_C [M_1]$	$\rho_C [M_2]$	$\rho_C [M_3]$
Length ^a	-0.194	-0.552	-0.582
Gene density ^b	-0.178	-0.076	-0.107
Inter-chromosomal duplications ^c	-0.330	-0.242	-0.165
Intra-chromosomal duplications ^c	-0.342	-0.248	-0.158
All pairwise duplications ^c	-0.331	-0.237	-0.149
Local composition A ^d	+0.658	+0.762	+0.461
Local composition T ^d	+0.668	+0.674	+0.551
Local composition C ^d	+0.021	+0.039	+0.269
Local composition G ^d	-0.149	+0.211	+0.246
Global composition AT ^e	+0.052	-0.154	-0.219

^aLengths are in the 2nd column of Table I

^bGene Density data are taken from Ref. 10, 11

^cInter- and Intra chromosomal duplications data are taken from Ref. 10

^dLocal base composition are shown in the 7th-10th columns in Table I for the first 10 MBases

^eData for global base composition are in Table I

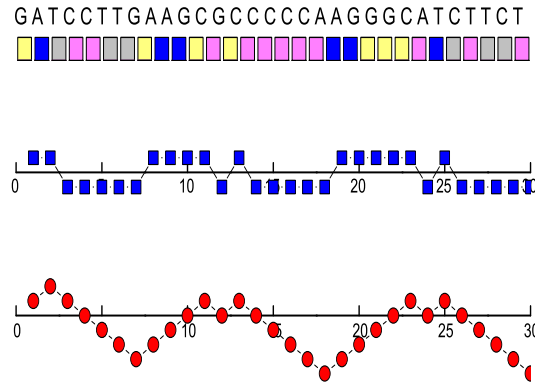


FIG. 3: Scheme of the first 30 bases sequence of the human chromosome 1. From Top to Bottom: nucleotide sequence; the corresponding +1 and -1 sequence; the DNA walk $y(x)$ obtained by summing the increments +1 and -1.

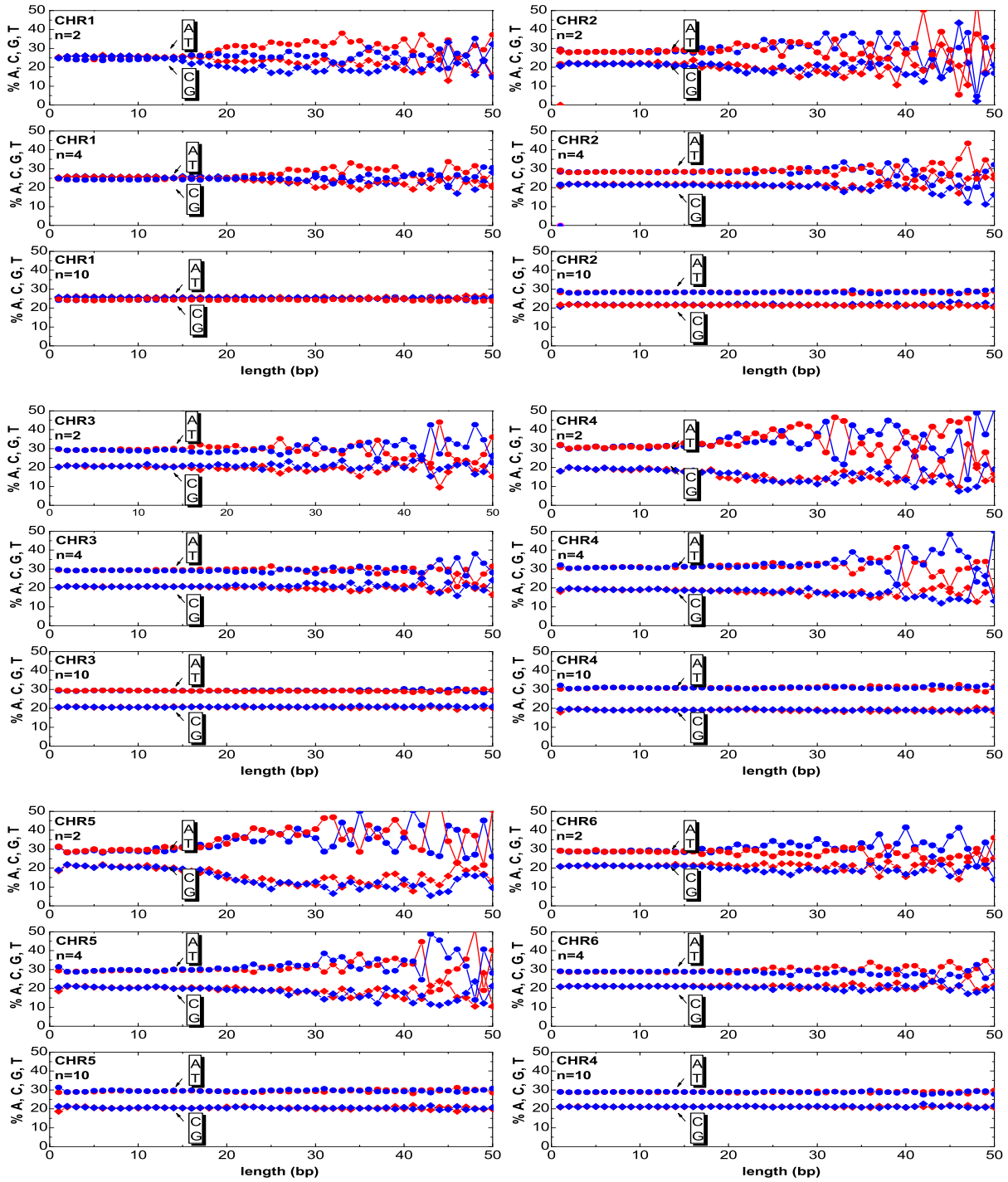


FIG. 4: Base composition (% of ATCG nucleotides) of the clusters in the human chromosomes 1, 2, 3, 4, 5, 6. For each chromosome, the plots refer to windows $n = 2$, $n = 4$, $n = 10$

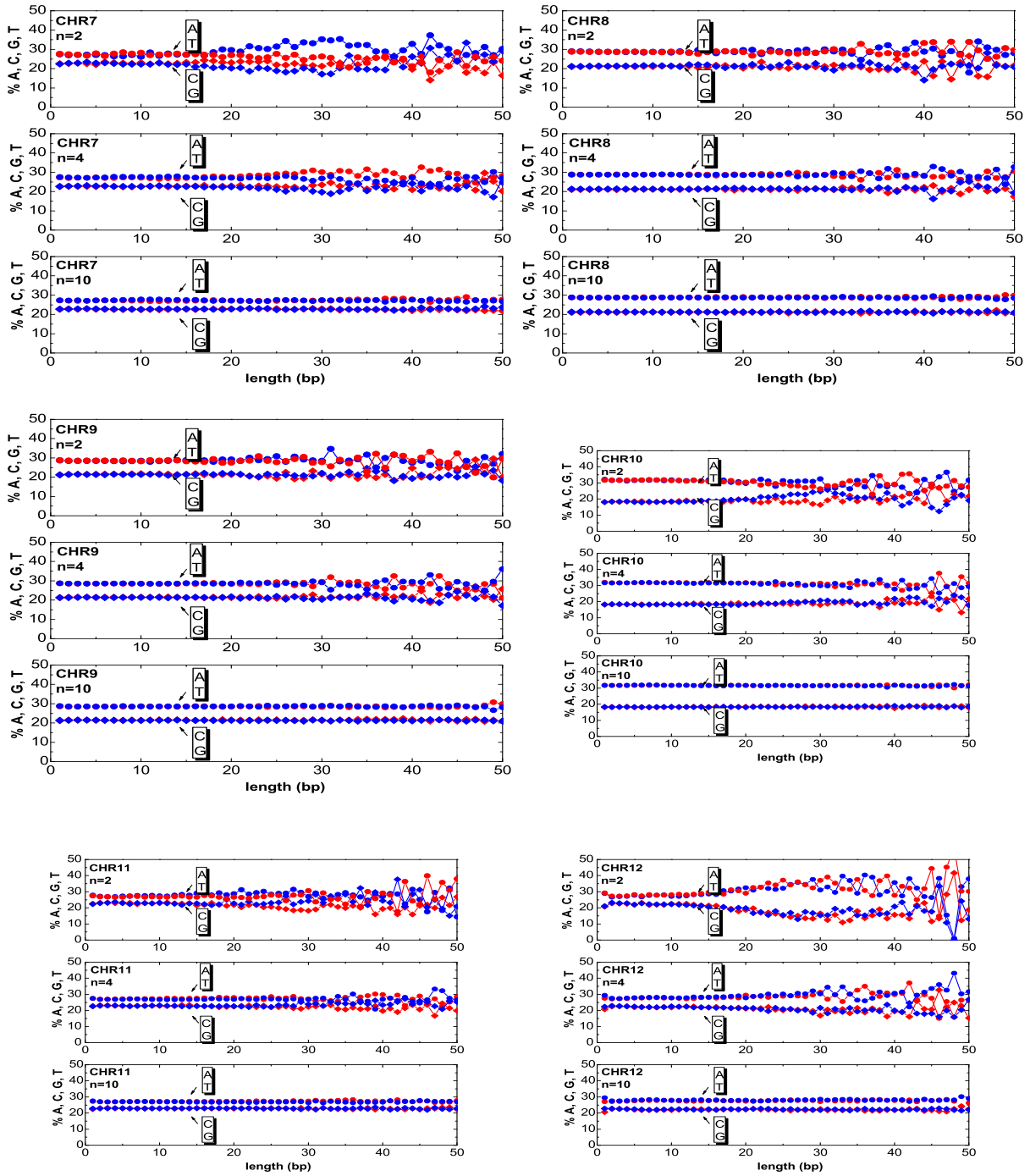


FIG. 5: Same as Fig.4 but for the chromosomes 7, 8, 9, 10, 11, 12.

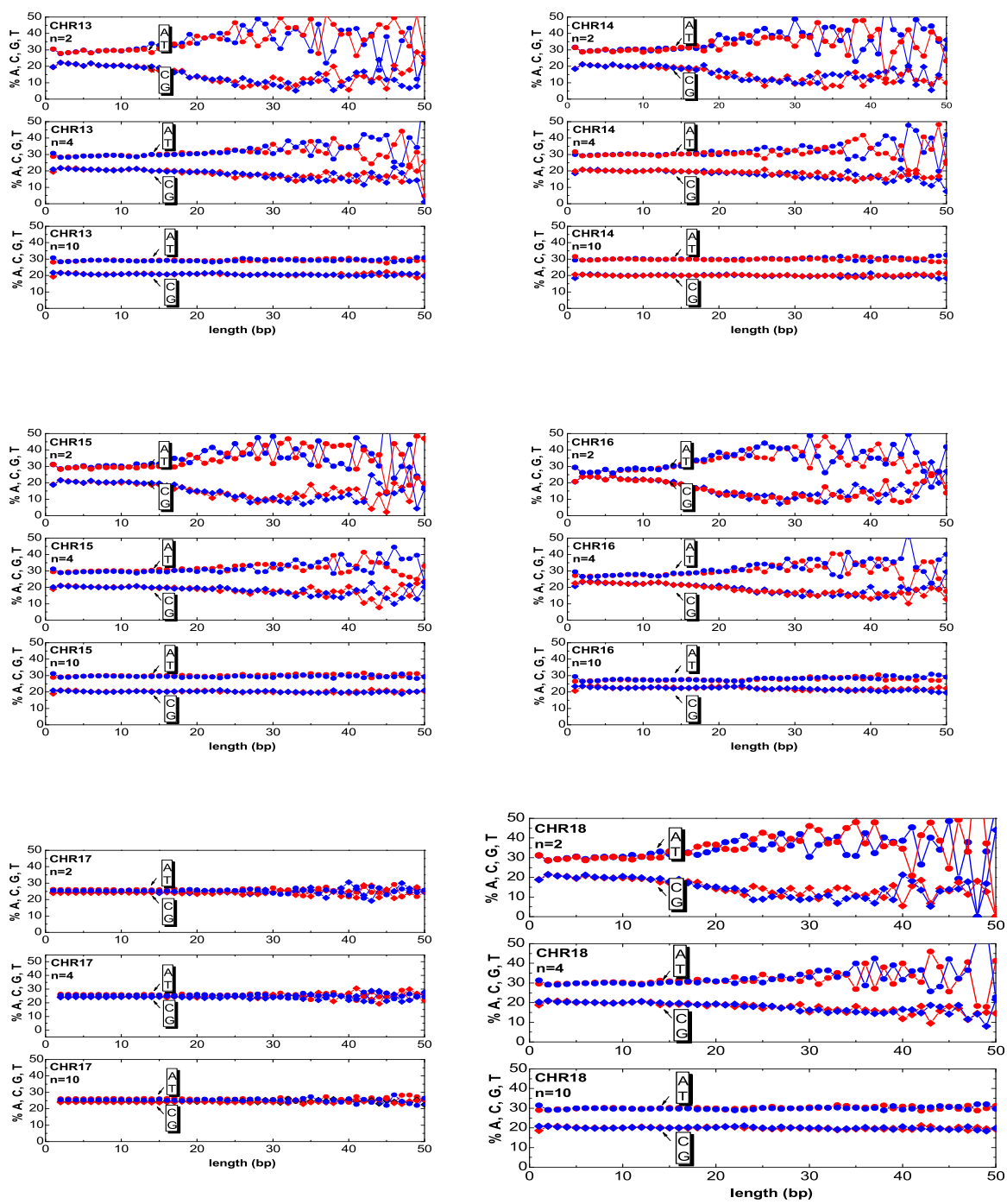


FIG. 6: Same as Fig.4 but for the chromosomes 13, 14, 15, 16, 17, 18.

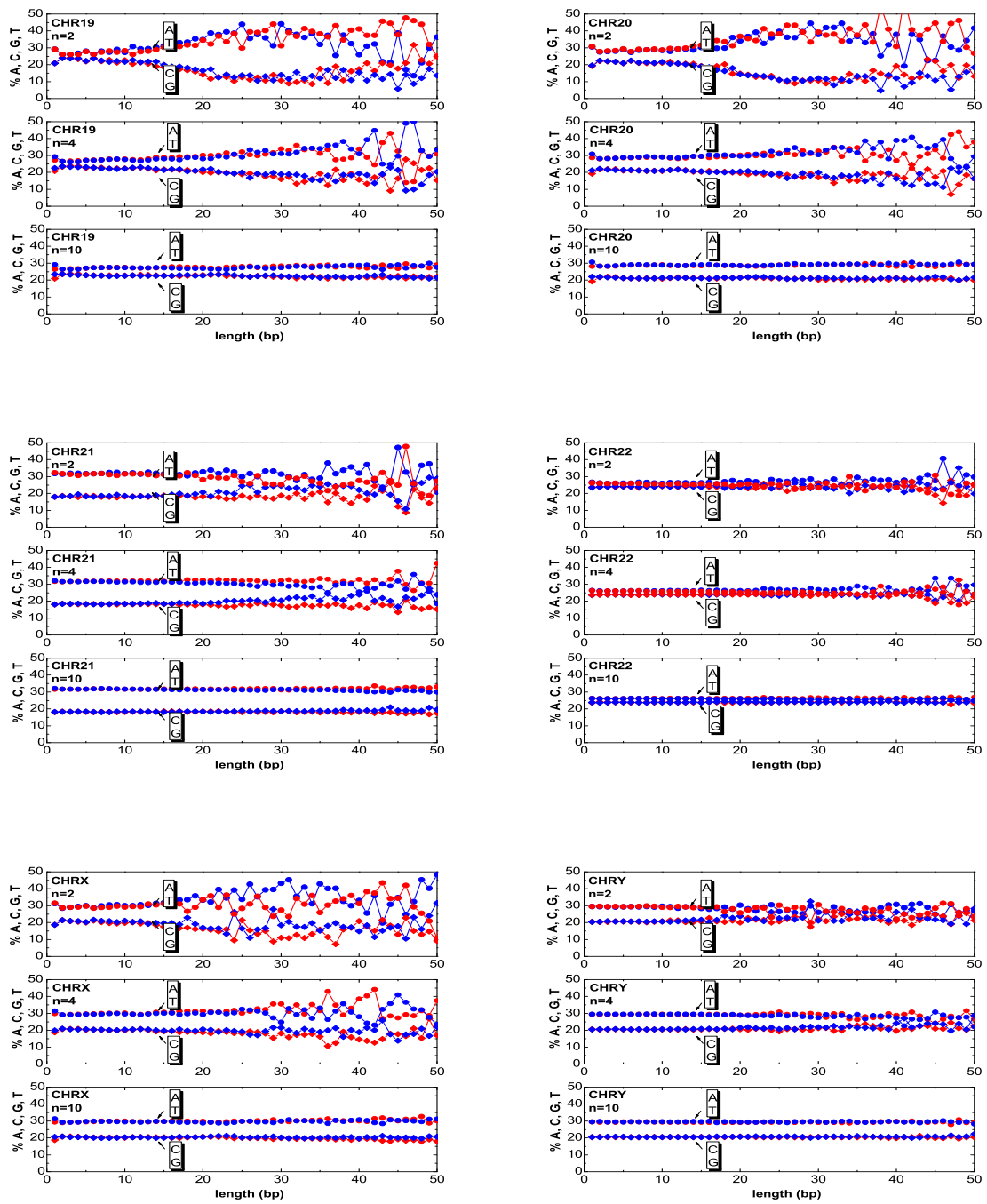


FIG. 7: Same as Fig.4 but for the chromosomes 19, 20, 21, 22, X, Y.